



The Biochemistry and Fidelity of Synthesis by the Apicoplast Genome Replication DNA Polymerase Pfpref from the Malaria Parasite *Plasmodium falciparum*

Scott R. Kennedy¹, Cheng-Yao Chen¹, Michael W. Schmitt¹, Cole N. Bower¹ and Lawrence A. Loeb^{1,2*}

¹Department of Pathology, University of Washington at Seattle, Seattle, WA 98195, USA

²Department of Biochemistry, University of Washington at Seattle, Seattle, WA 98195, USA

Received 16 March 2011;
received in revised form
15 April 2011;
accepted 27 April 2011

Edited by J. Karn

Keywords:
replication;
apicoplexan;
pIDNA;
Pom1

Plasmodium falciparum, the major causative agent of human malaria, contains three separate genomes. The apicoplast (an intracellular organelle) contains an ~35-kb circular DNA genome of unusually high A/T content (>86%) that is replicated by the nuclear-encoded replication complex Pfpref. Herein, we have expressed and purified the DNA polymerase domain of Pfpref [KPom1 (Klenow-like polymerase of malaria 1)] and measured its fidelity using a *LacZ*-based forward mutation assay. In addition, we analyzed the kinetic parameters for the incorporation of both complementary and noncomplementary nucleotides using KPom1 lacking 3'→5' exonucleolytic activity. KPom1 exhibits a strongly biased mutational spectrum in which T→C is the most frequent single-base substitution and differs significantly from the closely related *Escherichia coli* DNA polymerase I. Using *E. coli* harboring a temperature-sensitive polymerase I allele, we established that KPom1 can complement the growth-defective phenotype at an elevated temperature. We propose that the error bias of KPom1 may be exploited in the complementation assay to identify nucleoside analogs that mimic this base-mispairing and preferentially inhibit apicoplast DNA replication.

© 2011 Published by Elsevier Ltd.

Introduction

Plasmodium falciparum, the infectious agent associated with most cases of malaria, is responsible for an estimated 5 million deaths annually throughout the world.¹ This infectious parasite contains a nuclear genome and a mitochondrial genome, as well as a third unique genome that is encapsulated

in an organelle termed the apicoplast. The apicoplast, which is thought to be derived from the secondary endocytosis of photosynthetic algae, is involved in a variety of biosynthetic pathways and is required for parasite survival. The apicoplast contains its own plastid-derived ~35-kb closed circular double-stranded DNA genome (pIDNA) that is replicated by a bidirectional θ mechanism and segregated into daughter cells.^{2,3} The genome encodes several subunits of rRNA and the accompanying ribosomal proteins, 25 species of tRNA, an RNA polymerase, and several open reading frames coding for chaperones, as well as other proteins of unknown function.⁴

The biochemical and cellular processes involved in pIDNA replication are poorly understood;

*Corresponding author. Department of Pathology, University of Washington at Seattle, HSB K-072, Box 357705, 1959 Pacific Street NE, Seattle, WA 98125-7705, USA. E-mail address: laloeb@u.washington.edu.

Abbreviations used: Pol I, polymerase I; EDTA, ethylenediaminetetraacetic acid.

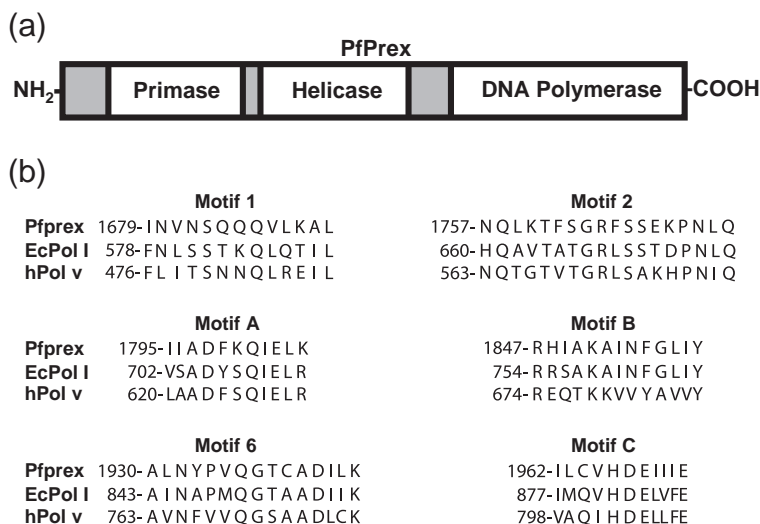


Fig. 1. (a) The domain organization of Pfpref. (b) Sequence comparison of the evolutionarily conserved DNA polymerase motifs of the *P. falciparum* Pfpref polymerase domain, *E. coli* DNA Pol I, and human Pol ν .

68 however, several proteins that are involved in DNA
69 metabolic processes are encoded by the nuclear
70 genome, synthesized in the cytoplasm, and trans-
71 ported to the apicoplast. These include a bacteria-
72 like gyrase, a DNA ligase, and several unclassified
73 open reading frames that are homologous to DNA
74 repair enzymes.^{5,6} Of these, the apicoplast gyrase is
75 a known target for inhibition by the drug cipro-
76 floxin, a major therapeutic agent for the treatment of
77 malaria, suggesting that other enzymes involved in
78 plDNA replication and maintenance may be useful
79 drug targets.⁷⁻¹⁰

80 Apicoplast DNA replication is catalyzed by the
81 nuclear-encoded apicoplast-targeted polyprotein
82 Pfpref, which is a large (2016 aa) multifunctional
83 peptide that contains three distinct domains that
84 exhibit DNA primase, DNA helicase, and DNA
85 polymerase activities, respectively¹¹ (Fig. 1a). The
86 helicase and primase segments are homologous to
87 T7 bacteriophage helicase and primase proteins.¹¹
88 The third domain contains a DNA polymerase that
89 is evolutionarily related to prokaryotic DNA
90 polymerase I (Pol I), an A-family polymerase,
91 based on sequence homology. Similar to DNA
92 polymerase γ , which is localized to the mitochon-
93 dria, Pfpref is believed to be the only DNA-
94 synthesizing enzyme in the apicoplast and is
95 thought to be involved in DNA replication, repair,
96 and recombination.

97 The three genomes present in *P. falciparum* (i.e.,
98 nuclear, mitochondrial, and plastidial) are among
99 the most A/T-rich yet sequenced genomes, with
100 plDNA being the richest (86.9% A/T).⁴ Given the
101 highly biased sequence composition of the apico-
102 plast genome, we asked if the plDNA polymerase
103 preferentially incorporated dATP and/or dTTP and
104 thus has a role in the maintenance of the A/T-rich
105 genome. To this end, we have expressed and
106 purified the DNA polymerase domain of Pfpref
107 [henceforth referred to as KPom1 (Klenow-like

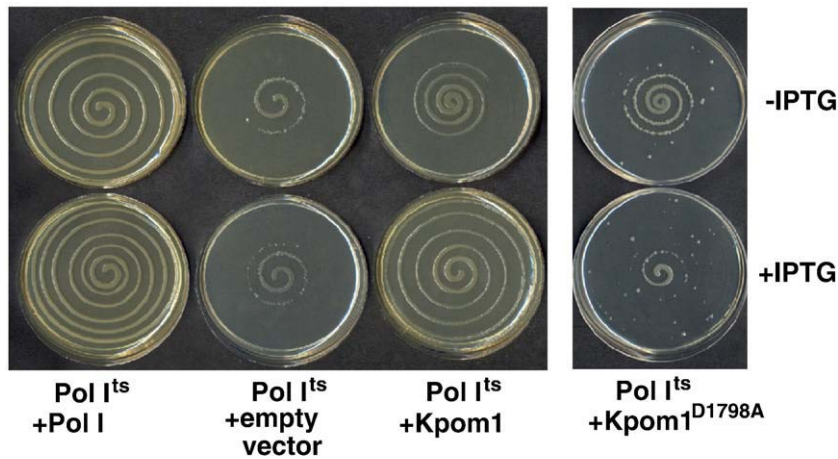
polymerase of malaria 1)] and have determined the
108 frequencies of misincorporations and the effects of
109 neighboring nucleotides using the M13mp2 forward
110 mutation assay for KPom1 with and without a
111 3' \rightarrow 5' exonucleolytic activity. In addition, we also
112 characterized the kinetics of incorporation of com-
113plementary and noncomplementary nucleotides.
114 Interestingly, we find that KPom1 exhibits a
115 strongly biased error spectrum, with the T \rightarrow C
116 single-base substitution being the most frequent,
117 and thus does not account for the maintenance of the
118 A/T-rich plastid genome. Even though the catalytic
119 site motifs are highly conserved between *Escherichia*
120 *coli* Pol I and KPom1, the spectrum of misincorpora-
121 tion by KPom1 is markedly different from that by *E.*
122 *coli* Pol I. This finding suggests that residues outside
123 of active-site motifs may influence the fidelity of
124 these two enzymes. Despite these differences, we
125 established that KPom1 is able to substitute for *E.*
126 *coli* Pol I *in vivo*. We suggest that the error bias of
127 KPom1 may be exploited in the complementation
128 assay to identify nucleoside analogs that mimic
129 base-mispairing and preferentially inhibit plDNA
130 replication. 131

132 Results

133 KPom1 can substitute for DNA polymerase Pol I 134 in *E. coli*

135 KPom1 is a member of the A-family of DNA
136 polymerases. There is a high degree of conservation
137 of amino acid sequences at the catalytic sites of DNA
138 polymerases; sequence alignment of KPom1 with *E.*
139 *coli* Pol I shows that all the required motifs for
140 polymerase activity in Pol I are present in KPom1
141 and are highly conserved (Fig. 1b). We have
142 previously shown that both mammalian Pol β ¹²

(a)



(b)

Pol I ^{ts}	+Pol I	+empty vector	+KPom1	+KPom1 ^{D1798A}
-IPTG (% relative growth)	100%	<0.001%	29%	<0.001%
+IPTG (% relative growth)	111%	<0.001%	60%	<0.001%

Fig. 2. Functional complementation of *E. coli* DNA Pol I by *P. falciparum* KPom1 *in vivo*. (a) *E. coli* JS200 cells were transformed with an empty pHSG576 vector or with a vector harboring Pol I, KPom1, or the KPom1^{D1798A} gene. (b) The complementation efficiency of Pol I^{ts} cells by exogenously expressed Pol I, KPom1, or KPom1^{D1798A} was quantified as described by Camps *et al.*¹⁴ The complementation efficiency of Pol I^{ts} cells by KPom1 or KPom1^{D1798A} was normalized to the conditions with Pol I in the absence of IPTG, which was set as 100%. Assays were performed in triplicate.

143 and human immunodeficiency virus reverse
 144 transcriptase¹³ can complement *E. coli* harboring a
 145 temperature-sensitive mutation in Pol I.^{12,13} To
 146 determine whether KPom1 can substitute for *E. coli*
 147 Pol I, we inserted KPom1 into an isopropyl β-D-1-
 148 thiogalactopyranoside (IPTG)-inducible vector and
 149 transformed it into *E. coli* that expresses a
 150 temperature-sensitive variant of Pol I, Pol I^{ts}. At
 151 37 °C, Pol I^{ts} is inactivated, and the strain is
 152 dependent on an exogenously supplied polymerase
 153 for colony formation. Figure 2a and b demonstrates
 154 that KPom1 almost fully restores wild-type growth
 155 when induced with IPTG. In the absence of IPTG, the
 156 KPom1-containing plasmid fails to form colonies at
 157 the nonpermissive temperature. In addition, essen-
 158 tially no growth is observed in vector-only control or
 159 when cells are transformed with a copy of KPom1
 160 harboring an active-site mutation (D1798A) that
 161 inactivates the polymerase (Fig. 2a and b).

162 KPom1 is error prone *in vivo*

163 We took advantage of the ability of KPom1 to
 164 substitute for the endogenous Pol I activity of *E. coli*
 165 in order to determine its *in vivo* fidelity. We utilized
 166 a two-plasmid system detailed by Camps *et al.*¹⁴ that
 167 uses a bacterial host, Pol I^{ts} (Fig. 3a).¹² In this system,
 168 one plasmid encodes the polymerase of interest
 169 (Klenow fragment of Pol I or KPom1 and its
 170 exonuclease-deficient derivatives), while the other
 171 contains the β-lactamase gene with an ochre (TAA)

172 mutation. Any mutation that results in a reversion of
 173 the ochre codon will lead to active β-lactamase
 174 activity and carbenicillin resistance. Thus, the
 175 frequency of bacteria rendered carbenicillin resistant
 176 reflects the frequency of ochre codon mutagenesis in
 177 the target plasmid.

178 Figure 3b shows the results for the *in vivo*
 179 reversion of mutations in β-lactamase by Klenow,
 180 Klenow^{exo-}, KPom1, and KPom1^{exo-}. The reversion
 181 frequencies for Klenow and Klenow^{exo-} are consis-
 182 tent with previous reports on β-lactamase reversion
 183 with this system.¹⁴ Specifically, the reversion fre-
 184 quency with Klenow^{exo-} is 4.5-fold greater than that
 185 observed with exonuclease-proficient Klenow and is
 186 consistent with previous reports.^{14,15} In JS200 strains
 187 expressing the KPom1 and KPom1^{exo-} enzymes, the
 188 reversion frequency is much higher than that of the
 189 corresponding controls. The KPom1 enzyme ex-
 190 hibits a 9-fold-higher reversion frequency than the
 191 Klenow fragment of *E. coli* Pol I. Surprisingly,
 192 KPom1^{exo-} exhibits an increase in the *in vivo*
 193 reversion frequency 793-fold relative to *E. coli* Pol
 194 I^{wt} and 41-fold higher than KPom1 (Fig. 3b), and
 195 suggests that the polymerase domain of KPom1 is
 196 very error prone and that the majority of polymerase
 197 mistakes are corrected by the exonuclease domain of
 198 the enzyme in the context of this system. Interest-
 199 ingly, the extremely high reversion frequency by
 200 KPom1^{exo-} occurs in the context of the A/T-rich
 201 TAA ochre codon, and the pDNA genome that this
 202 enzyme replicates is also A/T rich.

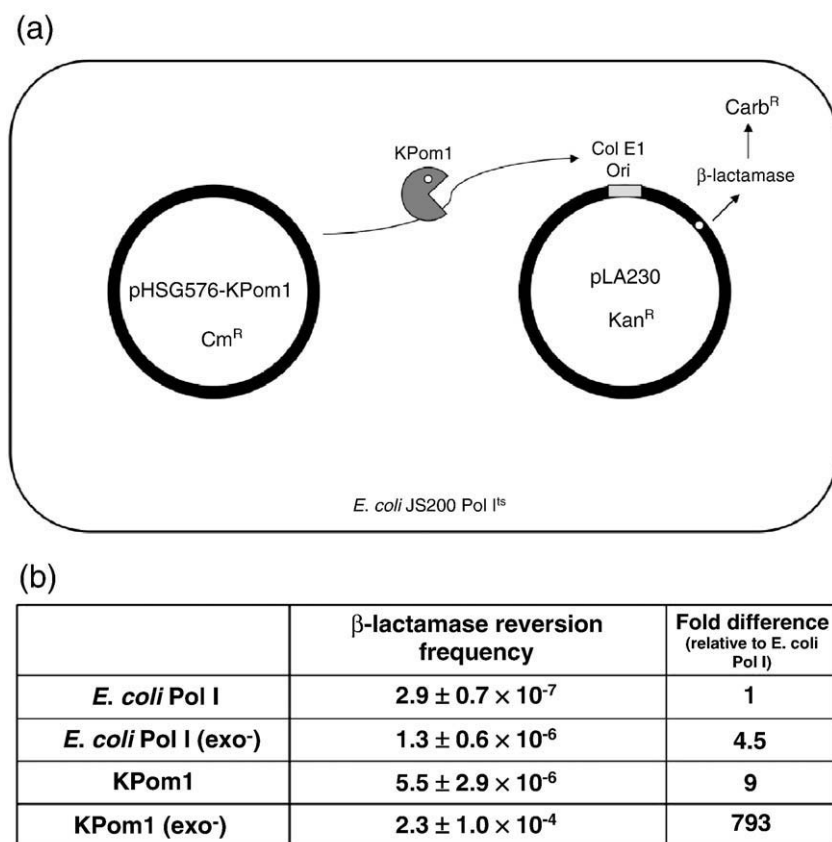


Fig. 3. *In vivo* fidelity of KPom1. (a) Schematic diagram of the two-plasmid β -lactamase reversion assay. JS200 (Pol I^{ts}) cells were transformed with two plasmids. Plasmid pHSG576 is a low-copy-number plasmid and carries the *polA* gene under the control of the *tac* promoter. The pLA230 plasmid carries the β -lactamase gene placed in close proximity downstream of a pUC19 (ColEI-type) origin of replication. The polymerase of interest is expressed from pHSG576 and initiates replication of pLA230. If the polymerase makes a misinsertion when copying the ochre codon, it will lead to a reversion of a functional β -lactamase enzyme. (b) Reversion frequencies for the β -lactamase reversion assay. The fold increase in the reversion frequency is relative to *E. coli* Pol I.

203 Biochemical characterization of KPom1

204 In order to determine if KPom1 exhibits a lower
 205 fidelity for nucleotide misinsertions opposite tem-
 206 plate dA or dT relative to template dC or dG, we
 207 used the purified enzyme to measure the *in vitro*
 208 fidelity and incorporation kinetics for all 16 possible
 209 base pairs. We were unable to express the apicoplast
 210 DNA polymerase in *E. coli* or yeast using different
 211 high-expression vectors. We reasoned that this lack
 212 of high expression could be due to the disparity in
 213 the codon usage bias between *P. falciparum* and *E.*
 214 *coli*. Therefore, we obtained a chemically synthesized
 215 gene, optimized for *E. coli* and coding for amino
 216 acids 1431–2016 of Pfpex (Supplementary Fig. 1),
 217 which corresponds to the Pol I-like DNA polymer-
 218 ase domain (KPom1). The expressed N-terminal
 219 maltose-binding domain fusion protein was purified
 220 to near homogeneity using a heparin column,
 221 followed by amylose resin (Supplementary Fig. 2).
 222 After cleavage and removal of the maltose-binding
 223 peptide, the purified DNA polymerase is highly
 224 active, with a specific activity of 77 pmol of dNMPs
 225 incorporated per minute per nanogram of protein
 226 for KPom1^{WT} and 53 pmol/min ng for KPom1^{exo-}.
 227 KPom1 exhibits maximal activity at ~ 10 mM Mg²⁺
 228 (Supplementary Fig. 3a) and pH 9.0 (Supplemen-
 229 tary Fig. 3b). Polymerase activity increases 2-fold
 230 from 18 °C to ~ 40 °C and then rapidly declines,

consistent with the idea that enzyme activity has
 evolved for DNA replication in warm-blooded
 animals (Supplementary Fig. 3c).

Fidelity of DNA synthesis by KPom1 DNA polymerase

The fidelity of DNA synthesis by the wild-type
 and exonuclease-deficient KPom1 DNA polymer-
 ases was determined using the M13mp2 forward
 mutation assay.¹⁶ The substrate is double-stranded
 M13mp2 with a 407-nucleotide single-stranded gap
 in the *LacZ α* gene. A purified DNA polymerase is
 used to fill in the single-stranded segment *in vitro*,
 which is then transformed into *E. coli* and plated on
 a lawn of α -complementation cells in the presence of
 5-bromo-4-chloro-3-indolyl- β -D-galactopyranoside
 and IPTG. Accurate synthesis by the polymerase
 results in the faithful replication of the *LacZ α* gene
 and the formation of dark-blue plaques, while
 polymerase errors yield light-blue or colorless
 plaques. The fidelity of the polymerase is deter-
 mined from the ratio of mutant to wild-type
 plaques; the error spectrum of the polymerase is
 determined by sequencing the resulting plaques.
 This assay allows for the monitoring of a broad range
 of mutations, including all 12 single-nucleotide
 misinsertion mutations and small insertion–deletion
 mutations, as well as short duplications, additions,

t1.2 **Table 1.** Mutation rates in the *LacZ* forward mutation assay

	Number of detectable sites	Wild type		Exo ⁻		
		Number detected	Error rate (×10 ⁻⁵)	Number detected	Error rate (×10 ⁻⁵)	
t1.4						
t1.3	Mispair					
t1.5	T-dTMP	16	0	0	≤0.4	
t1.6	T-dGMP	27	1	52	14	
t1.7	T-dCMP	23	0	0	≤0.3	
t1.8	C-dTMP	16	0	0	≤0.4	
t1.9	C-dAMP	25	2	4	1.1	
t1.10	C-dCMP	9	0	0	≤0.8	
t1.11	G-dTMP	22	0	10	3.2	
t1.12	G-dAMP	25	0	0	≤0.3	
t1.13	G-dGMP	19	0	0	≤0.4	
t1.14	A-dAMP	23	0	0	≤0.3	
t1.15	A-dGMP	17	0	0	≤0.4	
t1.16	A-dCMP	29	1	3	1.1	
t1.17	Base substitutions	125	4	69	3.9	
t1.18	+Insertions	199	0	5	0.2	
t1.19	-1 deletions	199	6	34	1.2	
t1.20	Large deletion ^a	Not defined	4	7	37	
t1.21	<i>LacZ</i> mutation frequency		1.3×10 ⁻³		6.3×10 ⁻³	
t1.22	^a For large deletions, mutation frequency is reported instead of the error rate.					

258 and rearrangements.¹⁶ With the 'wild-type' KPom1,
 259 only 14 phenotypic colonies (i.e., light-blue or
 260 colorless plaques) were observed in the 10,769
 261 observed colonies, resulting in a mutation frequency

t2.1 **Table 2.** Comparison of mutation rates between
t2.2 KPom1^{exo-} and other polymerases

	Error rate for single-base deletion (×10 ⁻⁵)	Error rate for single-base substitution (×10 ⁻⁵)
t2.3	DNA polymerase	
t2.4	Kpom1 (exo ⁻) ^a	3.9
t2.5	<i>E. coli</i> Klenow (exo ⁻) ^b	2.5
t2.6	<i>Taq</i> Pol (exo ⁻) ^c	1.7
t2.7	Human Pol ν ^d	350
t2.8	Human Pol θ ^e	240
t2.9	Human Pol γ (exo ⁻) (+p140 and p55) ^f	4.1
t2.10	Human Pol α ^g	7.5
t2.11	Human Pol δ (exo ⁻) ^h	4.4
Q6 t2.12	Yeast Pol ϵ (exo ⁻) ⁱ	24
t2.13	Human Pol β ^j	23
t2.14	Human Pol λ ^j	90
t2.15	Human Pol η ^k	3500
t2.16	Human Pol κ ^l	580

t2.17 ^a Error rates were derived from this study.

Q7 ^b Single-base deletions were adapted from Minnick *et al.* (1996), whereas single-base substitutions were adapted from Bebenek *et al.*¹⁵

t2.18 ^c Error rates were adapted from Eckert and Kunkel.¹⁷

t2.19 ^d Error rates were adapted from Arana *et al.*¹⁹

t2.20 ^e Error rates were adapted from Arana *et al.*²⁰

t2.21 ^f Single-base deletions were adapted from Longley *et al.*,¹⁸ whereas single-base substitutions were reported in Table 2 of

t2.22 Arana *et al.*¹⁹

t2.23 ^g Error rates are unpublished data reported in Table 2 of Arana *et al.*²⁰

t2.24 ^h Error rates were adapted from Schmitt *et al.*²¹

Q8 t2.25 ⁱ Error rates were adapted from Shcherbakova *et al.* (2003).

Q9 t2.26 ^j Error rates were adapted from Bebenek *et al.* (2003).

Q10 t2.27 ^k Error rates were adapted from Matsuda *et al.* (2000, 2001).

Q11 t2.28 ^l Error rates were adapted from Ohashi *et al.* (2000).

of 0.13%—less than 2-fold greater than the back- 262
 ground of the assay (0.07%).^{15,16} In contrast, with 263
 KPom1^{exo-}, 114 mutant plaques were detected in a 264
 total of 18,254 plaques, resulting in a mutation 265
 frequency of 0.63%. These mutation frequencies for 266
 both the wild type and the exonuclease-deficient 267
 KPom1 are similar to those observed for other high- 268
 fidelity A-family polymerases, including *E. coli* Pol 269
 I,¹⁵ *Taq* DNA polymerase,¹⁷ and human DNA 270
 polymerase γ .¹⁸ The presence of the exonuclease 271
 domain imparts at least a 6-fold increase in fidelity, 272
 thus showing that it is able to correct most 273
 misincorporation events that the polymerase active 274
 site makes. 275

The error spectrum of KPom1 was determined by 276
 sequencing the observed *lacZ* mutants and by 277
 tabulating the types and sequence contexts of the 278
 mutations. The results for both KPom1^{wt} and 279
 KPom1^{exo-} were used to calculate the error rates 280
 for each type of mutation (Fig. 4, Table 1), and the 281
 error spectrum of KPom1^{exo-} was compared to that 282
 of other characterized polymerases (Table 2). For 283
 KPom1^{exo-}, 39 of the 115 sequenced verified 284
 mutants were single-base insertion or deletions; 285
 the error rates were 1.2×10⁻⁵ and 0.2×10⁻⁵, 286
 respectively. Of the 34 detected -1 frameshift 287
 mutations found, 28 were in nucleotide repeats of 288
 two or more identical bases, consistent with a 289
 mechanism involving a template slippage event.²² 290

For KPom1^{exo-}, 69 of the 115 phenotypic mutants 291
 consisted of single-base substitutions—a base sub- 292
 stitution error rate of 3.9×10⁻⁵. Even though the 293
 M13mp2 forward mutation assay can detect all of 294
 the 12 single-base substitutions, only a subset was 295
 observed. Of the 69 sequenced single-base sub- 296
 stitutions, the majority (52/69 or 75%) were the 297
 result of a T→C transition (i.e., T:dGMP). The 298

Q1

299 frequency of this transition mutation was 14×10^{-5} ,
 300 three times greater than the frequency generated by
 301 the closely related *E. coli* Pol I^{exo-} (Fig. 4, Tables 1
 302 and 2).¹⁵ The second most common observed base
 303 substitution (10/69 or 14%) was the G→A (i.e., G:
 304 dTMP) transition, which occurs at a rate of
 305 3.2×10^{-5} —6-fold higher than what is observed for
 306 *E. coli* Pol I^{exo-}.¹⁵ Both C→T (C:dAMP) and A→G
 307 (A:dCMP) mutations occur at a rate of 1.1×10^{-5}
 308 and, combined, only account for 10% of the
 309 observed single-base substitutions. No other base
 310 substitutions were observed. This error spectrum
 311 deviates significantly from *E. coli* Pol I^{exo-}, even
 312 though these two enzymes share a significant
 313 sequence identity in their active-site motifs (Fig.
 314 1b) and have a similar overall error rate. Specifically,
 315 KPom1^{exo-} catalyzes primarily T→C transitions,
 316 while *E. coli* Pol I^{exo-} misincorporations result
 317 predominantly in C→T transitions, G→T transver-
 318 sions, and G→C transversions.¹⁵ In addition, a
 319 majority of T→C mutations (~65%) with KPom1^{exo-}
 320 DNA polymerase occurred in a sequence context in
 321 which the 5'-template base is either a C or a G. The
 322 mutation spectrum for KPom1^{exo-} is most similar to
 323 that of the A-family lesion bypass polymerase Pol ν
 324 (see Discussion for details).

325 Steady-state kinetics of KPom1

326 Examining the fidelity of KPom1 using steady-
 327 state kinetics gives an indication of which step in the
 328 nucleotide discrimination process is rate limiting for
 329 the incorporation of specific deoxynucleoside tri-
 330 phosphates. For example, a higher K_m would
 331 suggest that nucleotide discrimination is due to an
 332 increase in substrate dissociation (increase in k_{off}),
 333 while a lower V_{max} would indicate an unfavorable
 334 geometry of the bound nucleotide in the active

335 site.^{15,23} We used a steady-state gel-based assay to
 336 determine the apparent kinetic parameters (V_{max}
 337 and K_m) for the incorporation of the correct or
 338 incorrect nucleotide across all 16 possible base
 339 pairings. These values were then used to calculate
 340 the fidelity of KPom1^{exo-}.²³

341 KPom1^{exo-} efficiently incorporated dAMP, dCMP,
 342 dTMP, or dGMP across from their complementary
 343 template bases and discriminated against the incor-
 344 rect nucleotide for all possible nucleotide mis-
 345 matches (Table 3). The calculated values for the
 346 fidelity of nucleotide misinsertion range from
 347 4.6×10^{-3} (T:dGMP) to 2.6×10^{-5} (A:dCMP) (Table 3).
 348 Values for some mismatches could not be calculat-
 349 ed due to a lack of observable incorporation. The
 350 most prevalent misinsertions observed in the
 351 kinetic assay are the same as the mispairs with
 352 the lowest observed fidelity in the M13mp2
 353 forward mutation assay (Table 1). The apparent
 354 values for K_m ranged from a 325-fold increase to a
 355 3000-fold increase for incorrect *versus* correct
 356 incorporation, but did not vary substantially for
 357 the correct incorporation reactions. The mispairs
 358 that were the least frequent in the M13mp2
 359 forward mutation assay also exhibited a relatively
 360 high value for K_m (>1000 μ M), whereas base
 361 mispairs with the lowest fidelity tended to have
 362 much lower values of K_m . Specifically, the values
 363 for K_m were highest when the identity of the
 364 template base was dG or dC, or when base-pairing
 365 involved an incoming nucleotide with the same
 366 identity as the template base. Conversely, when the
 367 template base was dA or dT, the values of K_m were
 368 on the order of 2-fold to 3-fold lower than the
 369 values observed for dG or dC. This observation
 370 suggests that KPom1 uses a mechanism whereby
 371 nucleotide discrimination for certain base-base
 372 mispairs (namely template dG, template dC, and

t3.2 **Table 3.** Fidelity of single-nucleotide insertion by KPom1^{exo-}

t3.3	Base pair	K_m (μ M)	V_{max} (fmol/min)	V_{max}/K_m (fmol/ μ M min)	Fidelity ^a
t3.4	T-dAMP	1.6 ± 0.7	12.5 ± 0.7	7.8	1
t3.5	T-dTMP	ND ^b	ND ^b	—	—
t3.6	T-dGMP	521 ± 54	18.8 ± 0.6	0.0361	4.61×10^{-3}
t3.7	T-dCMP	648 ± 350	0.91 ± 0.13	0.0014	1.80×10^{-4}
t3.8	C-dGMP	0.36 ± 0.09	8.2 ± 0.4	22.8	1
t3.9	C-dTMP	1300 ± 450	0.81 ± 0.09	0.0006	2.74×10^{-5}
t3.10	C-dAMP	ND ^b	ND ^b	—	—
t3.11	C-dCMP	ND ^b	ND ^b	—	—
t3.12	G-dCMP	0.72 ± 0.09	10.4 ± 0.3	14.4	1
t3.13	G-dTMP	290 ± 120	3.2 ± 0.6	0.0110	7.64×10^{-4}
t3.14	G-dAMP	1450 ± 650	3.9 ± 0.7	0.0027	1.86×10^{-4}
t3.15	G-dGMP	2200 ± 620	3.0 ± 0.4	0.0014	9.44×10^{-5}
t3.16	A-dTMP	0.70 ± 0.15	11.4 ± 0.6	16.30	1
t3.17	A-dAMP	1500 ± 260	1.6 ± 0.2	0.0011	6.55×10^{-5}
t3.18	A-dGMP	264 ± 117	2.9 ± 0.2	0.0110	6.74×10^{-4}
t3.19	A-dCMP	885 ± 228	0.92 ± 0.15	0.0010	6.38×10^{-5}

t3.20 ^a Fidelity is defined as $(V_{max}/K_m)_{wrong}/(V_{max}/K_m)_{right}$.

t3.21 ^b The reaction was too slow to be determined.

373 pyr:pyr/pur:pur) involves poor binding (i.e., increased off-rate).
374

375 In contrast to the values of K_m , which exhibit an
376 increase in magnitude for all mismatches relative to
377 the correct base pair, the values for the apparent
378 V_{max} ranged from a 13.7-fold decrease to a 1.5-fold
379 increase for incorrect *versus* correct incorporation.
380 The apparent V_{max} values for the correct incorporation
381 reactions were very similar to one another,
382 regardless of the template base identity, while the
383 V_{max} values for most mismatch reactions varied in a
384 range of about 4-fold, regardless of the identity of
385 the template base. A notable exception is the T:
386 dGMP mispair, which surprisingly exhibits a V_{max}
387 higher than that of the correct base pair.

388 Taken together, it appears that, depending on the
389 template base identity, KPom1 uses two different
390 strategies for nucleotide discrimination. When the
391 identity of the template base is dG or dC, the
392 polymerase primarily discriminates between the
393 correct nucleotide and the incorrect nucleotide
394 based on a reduced occupancy of the active site
395 (i.e., the rate of dissociation is much faster than the
396 rate of incorporation). This is most likely due to the
397 inability of these mispairs to form stable hydrogen
398 bonds between the template and the substrate. This
399 is consistent with the idea that fidelity for template
400 dG and dC is mostly governed by substrate
401 dissociation. However, this observation is not the
402 case for the G:dTMP mispair, which exhibits a
403 reduced K_m , while the value of V_{max} for this
404 mismatch is unchanged relative to the other
405 mispairs. This observation suggests that, for this
406 base mismatch, the fidelity is increasingly governed
407 by the rate of product formation.

408 Interestingly, when the template base identity is
409 dA or dT, the values of K_m tend to be much lower
410 than those of dG or dC and only vary by less than
411 2-fold, while V_{max} exhibits a greater than 20-fold
412 variation (Table 3). This observation is consistent
413 with the fidelity of mismatches involving template
414 dA or dT, being governed mostly by the base-pair
415 geometry in the polymerase active site. As men-
416 tioned previously, the T:dGMP base pair has a
417 higher V_{max} than the correct base pair (Table 3) and
418 indicates that the V_{max} for this mismatch does not
419 contribute favorably to the fidelity and that the
420 increased fidelity is primarily due to substrate
421 dissociation.

422 Discussion

423 Pfpref is a multifunctional fusion protein tar-
424 geted to the apicoplast. Even though definitive
425 proof is lacking, it is believed to be responsible for
426 the replication of the apicoplast genome using a
427 DNA Pol-I-like domain. In addition, it may also
428 function in apicoplast DNA repair and other DNA

synthetic functions. Thus, its presence in the 429
apicoplast is somewhat reminiscent of mammalian 430
DNA polymerase γ , which is also nuclearly 431
encoded and has been shown to carry out a 432
variety of DNA synthetic functions in mitochon- 433
dria. Because the apicoplast is a unique and 434
required component of the malaria parasite, it 435
could serve as an important target for specifically 436
preventing or treating infections by the malaria 437
parasite. To this end, we have expressed and 438
purified—as well as present fidelity and kinetic 439
studies of—KPom1, the plastid-targeted replicative 440
DNA polymerase domain from the malaria para- 441
site *P. falciparum*. Our results show that the 442
polymerase domain of the apicoplast genome 443
replication enzyme replicates the genome with 444
high fidelity and has an overall fidelity similar to 445
other fidelity A-family polymerases. The high level 446
of fidelity stems from an efficient discrimination of 447
mismatch nucleotides at the active site, as well as 448
the presence of a 3'→5' exonuclease domain 449
involved in proofreading, which is efficient at 450
removing the vast majority of mutations caused 451
by misinsertion at the active site. 452

453 Characterization of the exonuclease-deficient form
of KPom1 reveals the 'spectrum' of errors intro- 454
duced by the polymerase. The frequencies of in- 455
sertions and deletions (indels) of only a few 456
nucleotides in length are similar to the evolution- 457
arily related *E. coli* DNA Pol I^{exo-}, as well as other 458
high-fidelity A-family polymerases.^{15,18} The finding 459
that these indels occur at nucleotide repeats suggests 460
that these mutations may be the result of a strand 461
slippage event.²² In addition to indels, single-base 462
substitutions at specific template positions may also 463
be caused by a strand slippage. The M13mp2 464
forward mutation assay shows that a majority of 465
the observed T→C mutations occur after a template 466
dG or a dC. Slippage events could lead to a transient 467
template misalignment, with the template dG or dC 468
remaining in the catalytic site, followed by incorpo- 469
ration of the 'correct' nucleotide (i.e., dCMP and 470
dGMP, respectively). Such a mechanism has been 471
suggested to occur for human Pol γ .²² 472

473 One of the most intriguing aspects of the KPom1
polymerase is the error spectrum for single-base 474
substitutions. The most frequent mutations ob- 475
served with both Klenow^{exo-} and KPom1^{exo-} are 476
T→C transitions; however, the error frequency for 477
T→C transitions is more than 3-fold greater during 478
copying with KPom1. The next most frequently 479
scored mutation for KPom1 is G→A, while with *E.* 480
coli DNA Pol I^{exo-}, C→T and G→C mutations are 481
the next most frequent base substitutions.¹⁵ The 482
active-site motifs in the polymerase sites for KPom1 483
and *E. coli* DNA Pol I are nearly identical, as is the 484
overall accuracy in DNA synthesis; therefore, in 485
accounting for the differences in the error spectrum, 486
it is likely that distant amino acids have a profound 487

effect on the types of misincorporations catalyzed at the polymerase site.

Of the DNA polymerases that have been analyzed using the M13mp2 forward mutation assay, the error spectrum of KPom1^{exo-} most closely resembles that of human Pol ν , an error-prone lesion bypass polymerase that lacks a proofreading exonuclease activity.¹⁹ While the frequency of misincorporation by human Pol ν is greater than KPom1^{exo-} (Table 2), Pol ν makes primarily G→A (G:dTMP) mutations, followed by T→C (T:dGMP) substitutions.¹⁹ In contrast, for KPom1, the primary mutations are T→C mutations, followed by G→A substitutions. When considering the flanking sequence immediately 5' to a mutation, it is interesting to note that G→A mutations by Pol ν are primarily preceded by a template dA or dT, while the T→C mutation of KPom1 is primarily preceded by a template dG or dC. These observations suggest that the interaction of a polymerase with the template DNA must also influence the incorporation of specific incorrect nucleotides.

The apicoplast genome base-pair composition is >86% A/T,⁴ yet the most frequent mutations produced by KPom1 are T→C transitions, both in the presence and in the absence of exonuclease activity. This finding would suggest that a genome with a higher G/C content would evolve over time, thus leading to an apicoplast genome with reduced A/T content. One possible explanation as to why a G/C bias is not observed may involve biased nucleoside pools within the parasite. *In vivo* studies have previously shown that the levels of adenosine and thiamine nucleosides are several times higher in the malaria parasite than are cytosine and guanine,²⁴ and studies have shown that, at a genomic level, there is a distinct trend in the mutational bias towards high A/T content in bacterial obligate endosymbiotes and parasites.^{25,26} This enzyme may have evolved to lower the K_m value for dGTP and dCTP due to their reduced availability in the pool. This idea is consistent with our observations that mismatches involving dGTP and dCTP tend to have a lower K_m . Therefore, the skewed mutational bias exhibited by KPom1 may be the result of a selective advantage that keeps the A/T content of the genome from becoming too skewed and reducing organismal fitness. An alternative possibility as to why a G/C bias is not observed is that the misincorporation bias at the level of the DNA polymerase could be compensated for by a mismatch repair process that preferentially removes dGMP mismatches in the newly replicated DNA strand. However, we are unaware of evidence for a mismatch repair system that functions in apicoplast DNA.

The unique error signature of KPom1 is a product of its specific structural features that govern fidelity. This begs the question as to why KPom1 has an error spectrum similar to that of human Pol ν even though

the amino acid sequence is more closely related to *E. coli* Pol I. A comparison of all six conserved polymerase motifs of KPom1, *E. coli* Pol I, and human Pol ν shows that there are no amino acids conserved between KPom1 and Pol ν that are not also conserved in *E. coli* Pol I (Fig. 1b). This suggests that these motifs are not the only ones that govern the substrate selection by DNA polymerases and that other structural features or amino acids in the enzyme are also likely to affect substrate selection. Indeed, several multi-amino-acid insertions flanking these conserved motifs in human Pol ν and Pol θ (another A-family bypass polymerase) have been implicated in its reduced fidelity, suggesting that the determinants of fidelity are not strictly confined to the conserved polymerase motifs.^{20,27,28}

Finally, our finding that KPom1 complements the *in vivo* activity of Pol I in *E. coli* will allow us to exploit genetic complementary for both structure-function studies and drug screening. Genetic complementation has been shown to facilitate the screening of large libraries of DNA polymerase mutants with random nucleotides at designated positions. An analysis of KPom1 mutants will be important in identifying amino residues that govern nucleotide selection and account for the unique substrate specificity. These mutants can then be compared to other A-family polymerases, as described previously.^{29,30}

The ability to substitute KPom1 for Pol I brings about the feasibility of using *E. coli* as a vehicle for evaluating the potency of DNA polymerase inhibitors in a high-throughput manner. Such a system has been used to sensitize *E. coli* to the antiviral compound AZT by complementing human immunodeficiency virus reverse transcriptase.¹³ The uniquely biased error spectrum of the KPom1 polymerase suggests that nucleoside analogs that exploit this bias as a method of terminating apicoplast DNA synthesis could be developed. Since the T→C error rate of KPom1 is much higher than that of human Pol δ or Pol ϵ , in the replicative DNA polymerases in the nucleus, the design of specific nucleoside analogs that take this fact into account will more specifically target the parasitic polymerases instead of the replicative polymerases, thus minimizing incorporation into the host genome.

Materials and Methods

Construction of recombinant plasmids

The pSH576 derivative plasmids pECpoll and pEC-poll-3'exo⁻ that carry the *E. coli* wild-type and 3'→5' exonuclease-deficient Pol I gene, respectively, were constructed as described previously.¹⁴ The synthetic codon-optimized KPom1 or exonuclease-deficient KPom1^{D1531A} (KPom1^{exo-}) genes (the amino acid numbering system is

602 based on full-length Pfpref; Integrated DNA Technolo- 661
 603 gies, Coralville, IA) (Supplementary Fig. 1) were cloned 662
 604 into the pMAL-c2X expression plasmid using the BamHI 663
 605 and HindIII sites. The pMAL-c2X vector encodes a 664
 606 maltose-binding protein moiety, which was fused to the 665
 607 polymerase gene to expedite purification. 666

608 Protein expression and purification

609 *E. coli* Rosetta2 cells (Novagen, EMD Chemicals) 670
 610 containing a pMAL-c2X-KPom1 plasmid were grown at 671
 611 37 °C in 3 L of LB medium containing 50 µg/mL 672
 612 carbenicillin and 30 µg/mL chloramphenicol. Protein 673
 613 expression was induced by the addition of 0.2 mM IPTG 674
 614 at an OD₆₀₀ of ~0.6. Cells were grown for an additional 675
 615 20 h at 21 °C and harvested by centrifugation. Cell pellets 676
 616 were resuspended in 30 mL of buffer A [20 mM Tris-HCl 677
 617 (pH 7.4), 1 mM DTT, 1 mM ethylenediaminetetraacetic 678
 618 acid (EDTA), 5% (wt/vol) glycerol, 2 mM benzamidine, 679
 619 500 µg/mL lysozyme, and 1 mM PMSF]+200 mM NaCl 680
 620 and incubated on ice for 1 h. The crude cell extract was 681
 621 sonicated and clarified by centrifugation at 15,000g for 682
 622 20 min (Supplementary Fig. S2, lane I). The supernatant 683
 623 was diluted with buffer A+200 mM NaCl to 50 mL and 684
 624 loaded onto an amylose column preequilibrated in buffer 685
 625 A. The column was then washed with 100 mL of buffer A 686
 626 +200 mM NaCl. KPom1 was eluted with 20 mL of buffer 687
 627 A +200 mM NaCl+20 mM maltose (Supplementary Fig. 2, 688
 628 lane II). The fractions containing KPom1 were pooled and 689
 629 directly diluted with an equal volume of buffer A without 690
 630 NaCl and loaded onto a heparin column preequilibrated 691
 631 in buffer A +100 mM NaCl. The column was washed with 692
 632 40 mL of the same buffer. KPom1 was eluted with 30 mL 693
 633 of buffer A+1 M NaCl. Column fractions (2 mL each) 694
 634 containing fusion maltose-binding protein-KPom1 pro- 695
 635 tein were pooled and dialyzed at 4 °C overnight against 696
 636 factor Xa cleavage buffer [20 mM Tris-HCl (pH 8.0), 2 mM 697
 637 CaCl₂, and 100 mM NaCl] and then concentrated using an 698
 638 Amicon filter unit (molecular weight cutoff, 30,000). The 699
 639 maltose-binding domain was cleaved by addition of factor 700
 640 Xa according to the manufacturer's protocol (New 701
 641 England Biolaboratories). After cleavage, the sample was 702
 642 diluted with 4 vol of buffer A and loaded onto an amylose 703
 643 column equilibrated with buffer A. The column was then 704
 644 washed with 15 mL of buffer A. The column flow-through 705
 645 (Supplementary Fig. 2, lane III) was directly diluted with 706
 646 an equal volume of buffer A without NaCl and loaded on a 707
 647 heparin column preequilibrated in buffer A +100 mM 708
 648 NaCl and washed with 20 mL of the same buffer. KPom1 709
 649 was eluted with 15 mL of buffer A+1 M NaCl. Column 710
 650 fractions (1 mL) containing KPom1 proteins were pooled 711
 651 and dialyzed at 4 °C overnight against enzyme storage 712
 652 buffer [20 mM Tris-HCl (pH 7.4), 1 mM DTT, 0.5 mM 713
 653 EDTA, 50 mM NaCl, 2 mM benzamidine, and 15% (wt/vol) 714
 654 glycerol] and concentrated using an Amicon filter unit 715
 655 (molecular weight cutoff, 30,000) (Supplementary Fig. 2, 716
 656 lane IV). The mutant KPom1^{exo-} protein was purified with 717
 657 the same protocol as the wild-type KPom1 preparation.

658 Two-plasmid β-lactamase reversion assay

659 The assay was performed as described previously.¹⁴
 660 Briefly, the Pol I^{ts} *E. coli* strain JS200 (SC-18 recA718 polA12

661 *uvrA155 trpE65 lon-11 sulA1*) harboring the reporter 662
 663 plasmid pLA230 was transformed with plasmids encod- 664
 665 ing the gene for either wild-type Pol I, Pol I^{exo-}, KPom1, or 666
 667 KPom1^{exo-}. The recombinant strains were cultured at 668
 669 30 °C for 18 h in LB containing 30 mg/mL kanamycin, 670
 671 12.5 mg/mL tetracycline, and 30 mg/mL chlorampheni- 672
 673 col. A 0.01 vol of the precultured broth was inoculated into 674
 675 fresh growth media, then cultured at 37 °C until an A₆₀₀ of 676
 677 1.0 had been attained. Cells were then plated onto 678
 679 prewarmed 2×YT agar plates supplemented with 680
 681 30 µg/mL kanamycin, 12.5 µg/mL tetracycline, and 682
 683 30 µg/mL chloramphenicol in the presence or in the 684
 685 absence of 100 µg/mL carbenicillin. After incubation at 686
 687 37 °C for 24 h, colonies were counted, and reversion 688
 689 frequencies were calculated as the ratio of carbenicillin- 689
 690 resistant colonies to total colonies. 691

692 Genetic complementation assay

693 The spiral assay for testing the genetic complementation 694
 695 of exogenously expressed *E. coli* Pol I and KPom1 DNA 696
 697 polymerases was conducted as described previously using 698
 699 the temperature-sensitive *E. coli* strain JS200.³¹ To quan- 700
 701 titatively determine the complementation efficiency of Pol 701
 702 I^{ts} cells by wild-type and KPom1 DNA polymerases, we 702
 703 plated ~1000 cells of JS200 harboring either pHSG576, 703
 704 pECpoll, pHSG576-KPom1, or pHSG576-KPom1^{D1798A} (a 704
 705 mutant lacking polymerase activity) on 2×YT agar plates 705
 706 containing tetracycline and chloramphenicol at 30 °C or 706
 707 37 °C. The complementation efficiency of each construct 707
 708 was determined as the ratio of viable colonies at 37 °C on 708
 709 2×YT agar plates to those at 30 °C on plates after the 24-h 709
 710 incubation.¹⁴ The results shown in all figures represent the 710
 711 average of three experiments carried out independently. 711

693 Polymerase activity assays

694 The DNA polymerase activity of all purified proteins 694
 695 was quantified using activated calf thymus DNA, as 695
 696 previously described.¹⁴ KPom1 and KPom1^{exo-} protein 696
 697 were assayed for 3'→5' exonuclease activity using a 697
 698 duplex 5'-[³²P]-labeled 27/36-mer DNA containing a 3'- 698
 699 terminal G:G mismatch. Reaction mixtures (10 µL) con- 699
 700 tained 10 nM 5'-[³²P]-labeled 27/36-mer DNA and 0.01 U 700
 701 of wild-type Klenow fragment (New England Biolabora- 701
 702 tories), exonuclease-deficient Klenow fragment (New 702
 703 England Biolaboratories), 20 nM KPom1, or KPom1^{exo-} 703
 704 protein in the appropriate reaction buffer. Reactions were 704
 705 incubated at 37 °C for 15 min, terminated by addition of 705
 706 10 µL of 2× gel loading buffer [100% formamide, 0.03% 706
 707 bromophenol blue (wt/vol), and 0.03% xylene cyanol 707
 708 (wt/vol)], and boiled at 95 °C for 5 min. Ten microliters of 708
 709 each reaction mixture was analyzed by electrophoresis on 709
 710 an 8 M urea/18% polyacrylamide gel. 710

711 M13 forward mutation assay

712 The M13mp2 gap-filling forward mutation assay was 712
 713 performed as described previously.¹⁶ Briefly, the gap-filling 713
 714 reaction (15 µL) was carried out in polymerase reaction 714
 715 buffer [25 mM Tris-HCl (pH 9.0), 1 mM DTT, 10 mM 715
 716 MgCl₂, and 50 mg/mL bovine serum albumin] containing 716

Q1

717 4 fmol of purified double-stranded bacteriophage M13mp2
 718 DNA with a 407-nucleotide single-stranded gap within the
 719 *lacZα* complementation target sequence, 5 pmol of purified
 720 KPom1 or KPom1^{exo-}, and 100 μM of each dNTP. Reactions
 721 were incubated at 37 °C for 10 min and terminated by the
 722 addition of EDTA to a concentration of 10 mM. The
 723 completion of gap-filling reactions was confirmed by
 724 agarose gel electrophoresis. Aliquots of gap-filling re-
 725 actions were transformed into MC1061 cells and plated
 726 on agar plates containing 5-bromo-4-chloro-3-indolyl-β-D-
 727 galactopyranoside, IPTG, and a lawn of CSH50 *E. coli* host
 728 cells. After incubation of plates at 37 °C for 16 h, the
 729 numbers of wild-type (dark blue) and mutant (light blue
 730 and white) plaques were scored. Mutant plaques were
 731 isolated and individually grown in liquid culture, and the
 732 M13mp2 DNA was isolated and sequenced using the
 733 sequencing primer 5'-TCGGAACCACCATCAAAC-3'.
 734 Error rates were calculated as previously described.³²

735 Single-nucleotide insertion kinetics

736 The primer extension reaction was performed to
 737 determine single-nucleotide insertion kinetics, as described
 738 previously.^{21,23} Briefly, the 5'-[³²P]-labeled 16-mer primer
 739 5'-CATGAAGTACAAGGAC-3' was annealed to a 1.5-fold
 740 molar excess of the template 36-mer 5'-GCATT-
 741 CAGTXGTCCTTGATGTCATG-3', where the 'X' in bold-
 742 face was either A, C, T, or G. Primer extension reactions
 743 (40 μL) were carried out in polymerase reaction buffer
 744 [25 mM Tris-HCl (pH 9.0), 1 mM DTT, 10 mM MgCl₂, and
 745 50 mg/mL bovine serum albumin] containing 10 nM ³²P-
 746 labeled primer/template DNA, 20 nM purified KPom1^{exo-},
 747 and indicated concentrations of dNTPs. Reactions were
 748 incubated at 37 °C from 1 min to 5 min. The time of each
 749 reaction was chosen based on prior experiments that were
 750 performed to determine single completed hit conditions,
 751 with less than 20% of the total primer extended.^{23,33}
 752 Reactions were terminated by adding 40 μL of 2× gel loading
 753 buffer [95% formamide, 15 mM EDTA, 0.05% (wt/vol)
 754 bromophenol blue, and 0.05% (wt/vol) xylene cyanol].
 755 Samples were boiled and loaded onto an 8 M urea/15%
 756 polyacrylamide gel for analysis by electrophoresis.

757 Supplementary materials related to this article can be
 758 found online at doi:10.1016/j.jmb.2011.04.071

760 Acknowledgements

761 This work was supported by National Institutes of
 762 Health grants R01CA115202, R01CA102029, and
 763 P01AG033061. We thank Eddie Fox and Sharath
 764 Balakrishna for their useful comments and discussion.

Q5

765 References

766 1. Snow, R. W., Guerra, C. A., Noor, A. M., Myint, H. Y.
 767 & Hay, S. I. (2005). The global distribution of clinical
 768 episodes of *Plasmodium falciparum* malaria. *Nature*,
 769 **434**, 214–217.

2. He, H. Y., Shaw, M. K., Pletcher, C. H., Striepen, B.,
 770 Tilney, L. G. & Roos, D. S. (2001). A plastid
 771 segregation defect in the protozoan parasite *Toxoplas-
 772 ma gondii*. *EMBO J.* **20**, 330–339. 773
3. Stanway, R. R., Witt, T., Zobiak, B., Aepfelbacher, M.
 774 & Heussler, V. T. (2009). GFP-targeting allows
 775 visualization of the apicoplast throughout the life
 776 cycle of live malaria parasites. *Biol. Cell*, **101**, 415–430. 777
4. Wilson, R. J. M., Denny, P. W., Preiser, P. R.,
 778 Rangachari, K., Roberts, K., Roy, A. *et al.* (1996).
 779 Complete gene map of the plastid-like DNA of the
 780 malaria parasite *Plasmodium falciparum*. *J. Mol. Biol.*
 781 **261**, 155–172. 782
5. Dahl, E. L. & Rosenthal, P. J. (2008). Apicoplast
 783 translation, transcription and genome replication:
 784 targets for antimalarial antibiotics. *Trends Parasitol.*
 785 **24**, 243–284. 786
6. Kumar, A., Tanveer, A., Biswas, S., Ram, E. V. S. R.,
 787 Gupta, A., Kumar, B. & Habib, S. (2010). Nuclear-
 788 encoded DnaJ homologue of *Plasmodium falciparum*
 789 interacts with replication *ori* of the apicoplast genome.
 790 *Mol. Microbiol.* **75**, 942–956. 791
7. Ram, E. V. S. R., Kumar, A., Biswas, S., Kumar, A.,
 792 Chaubey, S., Siddiqi, M. I. & Habib, S. (2007). Nuclear
 793 *gyrB* encodes a functional subunit of the *Plasmodium*
 794 *falciparum* gyrase that is involved in apicoplast DNA
 795 replication. *Mol. Biochem. Parasitol.* **154**, 30–39. 796
8. Dahl, E. L. & Rosenthal, P. J. (2007). Multiple
 797 antibiotics exert delayed effects against the *Plasmodi-
 798 um falciparum* apicoplast. *Antimicrob. Agents Chem-
 799 mother.* **51**, 3485–3490. 800
9. Dahl, E. L., Shock, J. L., Shenai, B. R., Gut, J., DeRisi, J. L.
 801 & Rosenthal, P. J. (2006). Tetracyclines specifically
 802 target the apicoplast of the malaria parasite *Plasmodium*
 803 *falciparum*. *Antimicrob. Agents Chemother.* **50**, 3124–3131. 804
10. Goodman, C. D., Su, V. & McFadden, G. I. (2007). The
 805 effects of anti-bacterials on the malaria parasite *Plasmo-
 806 dium falciparum*. *Mol. Biochem. Parasitol.* **152**, 181–191. 807
11. Seow, F., Sato, S., Janssen, C. S., Riehle, M. O.,
 808 Mukhopadhyay, A., Phillips, R. S. *et al.* (2005). The
 809 plastidic DNA replication enzyme complex of
 810 *Plasmodium falciparum*. *Mol. Biochem. Parasitol.* **141**,
 811 145–153. 812
12. Sweasy, J. B. & Loeb, L. A. (1992). Mammalian DNA
 813 polymerase β can substitute for DNA polymerase I
 814 during DNA replication in *Escherichia coli*. *J. Biol.*
 815 *Chem.* **267**, 1407–1410. 816
13. Kim, B. & Loeb, L. A. (1995). Human immunodeficiency
 817 virus reverse transcriptase substitutes for DNA
 818 polymerase I in *Escherichia coli*. *Proc. Natl Acad. Sci.*
 819 *USA*, **92**, 684–688. 820
14. Camps, M., Naukkarinen, J., Johnson, B. P. & Loeb,
 821 L. A. (2003). Targeted gene evolution in *Escherichia*
 822 *coli* using a highly error-prone DNA polymerase I.
 823 *Proc. Natl Acad. Sci. USA*, **100**, 9727–9732. 824
15. Bebenek, K., Joyce, C. M., Fitzgerald, M. P. & Kunkel,
 825 T. A. (1990). The fidelity of DNA synthesis catalyzed
 826 by derivatives of *Escherichia coli* DNA polymerase I.
 827 *J. Biol. Chem.* **265**, 13878–13887. 828
16. Bebenek, K. & Kunkel, T. (1995). Analyzing fidelity of
 829 DNA polymerases. *Methods Enzymol.* **262**, 217–232. 830
17. Eckert, K. A. & Kunkel, T. A. (1990). High fidelity
 831 DNA synthesis by the *Thermus aquaticus* DNA
 832 polymerase. *Nucleic Acids Res.* **18**, 3739–3752. 833

- 834 18. Longley, M. J., Nguyen, D., Kunkel, T. A. & Copeland,
835 W. C. (2001). The fidelity of human DNA polymerase
836 γ with and without exonucleolytic proofreading
837 and the p55 accessory subunit. *J. Biol. Chem.* **276**,
838 38555–38562.
- 839 19. Arana, M. E., Takata, K. I., Garcia-Diaz, M., Wood, R. D.
840 & Kunkel, T. A. (2007). A unique error signature for
841 human DNA polymerase ν . *DNA Repair*, **6**, 213–223.
- 842 20. Arana, M. E., Seki, M., Wood, R. D., Rogozin, I. B. &
843 Kunkel, T. A. (2008). Low-fidelity DNA synthesis by
844 human DNA polymerase theta. *Nucleic Acids Res.* **36**,
845 3847–3856.
- 846 21. Schmitt, M. W., Matsumoto, Y. & Loeb, L. A. (2009).
847 High fidelity and lesion bypass capability of human
848 DNA polymerase δ . *Biochimie*, **91**, 1163–1172.
- 849 22. Bebenek, K. & Kunkel, T. A. (2000). Streisinger
850 revisited: DNA synthesis errors mediated by substrate
851 misalignments. *Cold. Spring Harbor Symp. Quant. Biol.*
852 **65**, 81–92.
- 853 23. Boosalis, M. S., Petruska, J. & Goodman, M. F. (1987).
854 DNA polymerase insertion fidelity—gel assay for site-
855 specific kinetics. *J. Biol. Chem.* **262**, 14689–14696.
- 856 24. Dyke, K. V., Trush, M. A., Wilson, M. E. & Stealey, P. K.
857 (1977). Isolation and analysis of nucleotides from
858 erythrocyte-free malarial parasites (*Plasmodium ber-*
859 *ghet*) and potential relevance to malaria chemotherapy.
860 *Bull. World Health Organ.* **55**, 253–264.
- 861 25. Hershberg, R. & Petrov, D. M. (2010). Evidence that
862 mutation is universally biased towards AT in bacteria.
863 *PLOS Genet.* **6**, e1001115.
- 864 26. Mann, S. & Chen, Y. P. P. (2010). Bacterial genomic
865 G+C composition-eliciting environmental adapta-
866 tion. *Genomics*, **95**, 7–15.
- 867 27. Takata, K. I., Arana, M. E., Seki, M., Kunkel, T. A. &
868 Wood, R. D. (2010). Evolutionary conservation of
869 residues in vertebrate DNA polymerase N conferring
870 low fidelity and bypass activity. *Nucleic Acids Res.* **38**,
871 3233–3244.
- 872 28. Hogg, M., Seki, M., Wood, R. D., Doublé, S. &
873 Wallace, S. S. (2011). Lesion bypass activity of DNA
874 polymerase θ (POLQ) is an intrinsic property of the
875 pol domain and depends on unique sequence inserts.
876 *J. Mol. Biol.* **405**, 642–652.
- 877 29. Loh, E., Choe, J. & Loeb, L. A. (2007). Highly tolerated
878 amino acid substitutions increase the fidelity of
879 *Escherichia coli* DNA polymerase I. *J. Biol. Chem.* **282**,
880 1201–12209.
- 881 30. Patel, P. H. & Loeb, L. A. (2000). DNA polymerase
882 active site is highly mutable: evolutionary conse-
883 quences. *Proc. Natl Acad. Sci. USA*, **97**, 5095–5100.
- 884 31. Shinkai, A. & Loeb, L. A. (2001). *In vivo* mutagenesis by
885 *Escherichia coli* DNA polymerase I Ile⁷⁰⁹ in motif A
886 functions in base selection. *J. Biol. Chem.* **276**, 46759–46764.
- 887 32. Glick, E., Anderson, J. P. & Loeb, L. A. (2002). *In vitro*
888 production and screening of DNA polymerase η mutants
889 for catalytic diversity. *BioTechniques*, **33**, 1136–1144.
- 890 33. Creighton, S., Bloom, L. B. & Goodman, M. F. (1995).
891 Gel fidelity assay measuring nucleotide misinsertion,
892 exonucleolytic proofreading, and lesion bypass effi-
893 ciencies. *Methods Enzymol.* **262**, 232–256.